Small noncoding RNA interactome capture reveals pervasive, carbon source–dependent tRNA engagement of yeast glycolytic enzymes

CLAUDIO ASENCIO, THOMAS SCHWARZL, SUDEEP SAHADEVAN, and MATTHIAS W. HENTZE

European Molecular Biology Laboratory, 69117 Heidelberg, Germany

ABSTRACT

Small noncoding RNAs fulfill key functions in cellular and organismal biology, typically working in concert with RNA-binding proteins (RBPs). While proteome-wide methodologies have enormously expanded the repertoire of known RBPs, these methods do not distinguish RBPs binding to small noncoding RNAs from the rest. To specifically identify this relevant subclass of RBPs, we developed small noncoding RNA interactome capture (snRIC$_{2C}$) based on the differential RNA-binding capacity of silica matrices (2C). We define the *S. cerevisiae* proteome of nearly 300 proteins that specifically binds to RNAs smaller than 200 nt in length (snRBPs), identifying informative distinctions from the total RNA-binding proteome determined in parallel. Strikingly, the snRBPs include most glycolytic enzymes from yeast. With further methodological developments using silica matrices, 12 tRNAs were identified as specific binders of the glycolytic enzyme GAPDH. We show that tRNA engagement of GAPDH is carbon source–dependent and regulated by the RNA polymerase III repressor Maf1, suggesting a regulatory interaction between glycolysis and RNA polymerase III activity. We conclude that snRIC$_{2C}$ and other 2C-derived methods greatly facilitate the study of RBPs, revealing previously unrecognized interactions.

Keywords: snRIC$_{2C}$; small noncoding RNA binding proteome; GAPDH; glycolytic enzymes; tRNA

INTRODUCTION

RNA–protein interactions govern not only gene expression from beginning to end, but are also crucial for the function of cellular machines such as the ribosome, the spliceosome, the signal recognition particle, telomerase, and many others (Glisovic et al. 2008; Gerstberger et al. 2014; Mitchell and Parker 2014; Singh et al. 2015). Recent work suggests that the biological scope of RNA–protein interactions and RNA-binding proteins (RBPs) is even larger than previously anticipated (Baltz et al. 2012; Castello et al. 2012). Against this background, the development of methods to study RNA–protein interactions and RBPs promises fundamental new insights.

Decades ago, UV photo-cross-linking was shown to catalyze covalent bond formation between RNA and proteins at zero distance (Hockensmith et al. 1986; Brimacombe et al. 1988) without similarly promoting protein–protein cross-linking (Greenberg 1979; Pashev et al. 1991; Suchanek et al. 2005). To identify the poly(A) RNA-binding proteome of cultured cells comprehensively, RNA interactome capture (RIC) combined UV photo-cross-linking with oligo(dT) capture of polyadenylated RNAs followed by mass spectrometry (Baltz et al. 2012; Castello et al. 2012). RIC was subsequently refined by introduction of locked nucleic acid (LNA)-modified dT-capture probes (enhanced RIC, eRIC), allowing more stringent conditions and improving the signal to noise ratio of conventional RIC (Perez-Perri et al. 2018, 2021). However, both RIC and eRIC only identify RBPs that bind polyadenylated RNAs. To identify RBPs irrespective of the class of RNAs that they bind to, OOPS (Queiroz et al. 2019) and XRNAX (Trendel et al. 2019) were developed to extract cross-linked RBPs from the interphase between aqueous and organic solvents after a phenol extraction of RNA, while the PTex method uses two organic solvents (Urdaneta et al. 2019).

We (Asencio et al. 2018) and others (Shchepachev et al. 2019) recently reported that the silica matrices commonly used for total RNA isolation also retain RBPs that are covalently cross-linked to RNA, a method we refer to as complex capture (2C). Here, we explored 2C for the determination of the total RNA-binding proteome of the yeast *Saccharomyces cerevisiae*, establishing RIC$_{2C}$.

Corresponding author: hentze@embl.org

Article is online at http://www.rnajournal.org/cgi/doi/10.1261/rna.079408.122. Freely available online through the *RNA* Open Access option.

Unexpected observations then motivated the development of further downstream applications of 2C, especially for the identification of the cellular RNAs that bind to an RBP of interest ($CLIP_{2C}$) and the determination of those RBPs that bind to small noncoding RNAs ($snRIC_{2C}$), a polyfunctional class of RNAs with multiple regulatory roles. These technical advances led us to uncover a novel connection between tRNAs, glycolytic enzymes and carbon metabolism in yeast.

RESULTS

RIC_{2C} identifies 983 RBPs in yeast

We recently reported that commercially available silica columns used to purify RNA can also be used for the copurification of cross-linked RBPs to capture covalently linked RNA–protein complexes, called complex capture (2C) (Asencio et al. 2018). To utilize 2C for the determination of a high confidence RNA-binding proteome of the yeast *Saccharomyces cerevisiae*, we irradiated cultured cells with 3 J/cm^2 UV light at 254 nm, using nonirradiated cells as negative controls. Lysates from three independent biological replicates were subjected to a first round of 2C purification. To minimize residual contamination with DNA-binding proteins, we treated the 2C eluates with DNase I and conducted a second round of 2C. Subsequently, RBPs in the second-round eluates were released by RNase I treatment, TMT-labeled, and analyzed by mass spectrometry (Fig. 1A). The enrichment of RBPs by RIC_{2C} compared to the negative controls is strong and highly consistent (Supplemental Fig. 1), identifying 983 RBPs from yeast (Fig. 1B; Supplemental Table 1). Gene Ontology (GO) term enrichment analysis confirms ribosomal proteins as a highly enriched category in the cross-linked samples, reflecting that RIC_{2C} is not restricted to mRNA-binding proteins and efficiently captures the total RNA binding proteome (Fig. 1C).

Comparison with published data sets of RBPs in yeast suggests that the repertoire of RBPs in yeast may be nearing completion, with 174 additional novel RBPs (Fig. 1D) identified in our data set, including 156 RBPs without known RNA-binding domains (RBD) (Fig. 1E). Like previous studies, RIC_{2C} identified numerous metabolic enzymes, including several members of the glycolytic pathway, as RBPs (Fig. 1B,E; Supplemental Table 1).

To validate RIC_{2C}, eluates from cross-linked and non-cross-linked samples were treated with RNase I or left untreated, and subjected to immunoblotting for the RBPs Pab1 and GAPDH (Tdh3), respectively. Both proteins were only retained by RIC_{2C} after cross-linking. Furthermore, Pab1 showed the characteristic RNA-induced smear that collapses after RNase treatment into more defined bands just exceeding the molecular mass of the native protein (Fig. 1F, top panel). Interestingly, cross-linked GAPDH shows a far more defined band of slower migration rather than a smear without RNase treatment, which again collapses into a faster migrating GAPDH band after RNA digestion (Fig. 1F, bottom panel). GAPDH has been found to bind tRNAs in HeLa cells (Singh and Green 1993), and our results reveal that yeast GAPDH apparently binds a relatively homogenous class of low molecular mass RNAs. These results suggest that yeast GAPDH may also bind tRNAs and exemplify the utility of RIC_{2C}.

$CLIP_{2C}$ identifies several tRNAs as specific GAPDH-binding partners

To follow up on the striking GAPDH result, we decided to determine its RNA binding partners. Existing CLIP protocols have been very successful with canonical RBPs like hnRNPs, splicing factors or Pab1 (Baejen et al. 2014), but show limitations with noncanonical RBPs, where often only a minor fraction of the cellular protein is bound to RNA. Such a situation typically causes signal to noise issues from a high background.

We reasoned that enrichment of the RNA-bound fraction by 2C before immunoprecipitation could help to address this situation. To test this notion, we compared GAPDH immunoprecipitations from input lysates and 2C eluates and evaluated the efficiencies of capturing cross-linked GAPDH–RNA complexes. Input and unbound fractions, together with eluates from the IPs were analyzed by western blotting. While the IP from the input lysate showed a stronger overall signal, including more background above and below the expected size, the pattern was unaffected by RNase treatment, strongly suggesting that most of the immunoprecipitated protein was not bound to RNA (Supplemental Fig. 2). In contrast, 2C extraction reduced the overall IP signal, but a shifted band became clearly visible above the size of native GAPDH in the sample not treated with RNase. This shifted band is RNase-sensitive and the signal accumulates at the expected size of GAPDH following RNA digestion (Supplemental Fig. 2). These results clearly show that 2C strongly enriches for the RNA-bound forms of GAPDH for immunoprecipitation, potentially improving the signal to noise ratio of subsequent sequencing experiments.

Encouraged by this result, we developed $CLIP_{2C}$ to identify the RNAs bound to GAPDH. Following a first round of 2C, the eluates were DNase I–treated and RNA was fragmented. A small aliquot was saved for sequencing an input sample, while the rest was used for immunoprecipitation. Libraries from the input and the RNA isolated from the immunoprecipitation were generated and sequenced (Fig. 2A). To test the 2C-CLIP method, we used Pab1-TAP and Tdh3-Protein A tagged strains to be used in IgG-based pulldowns. An untagged WT strain was also included in the experiment as a negative control (Supplemental Fig. 3). Sequencing data from the input

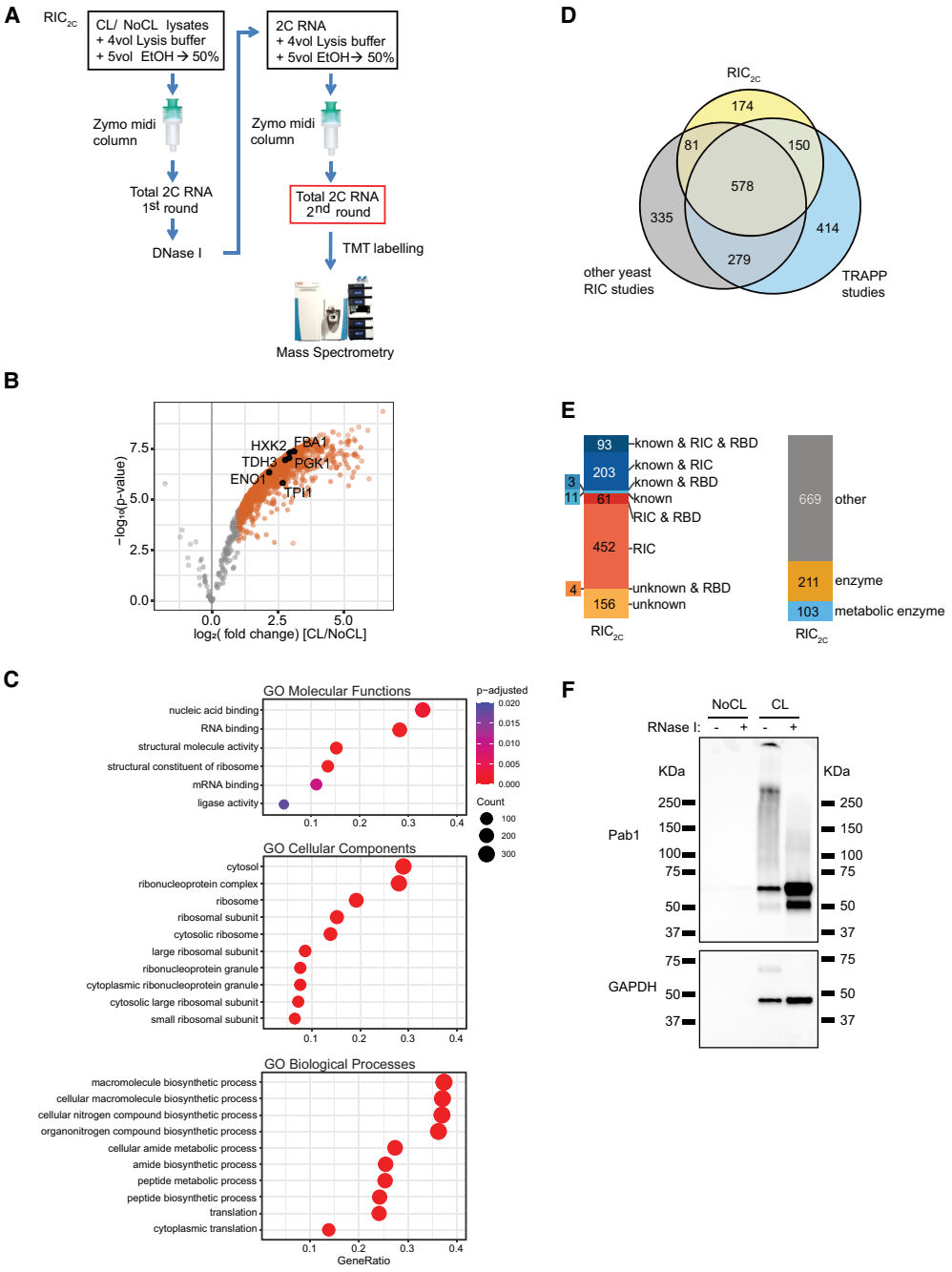

FIGURE 1. 2C total RNA interactome capture (RIC_{2C}) identified 983 RBPs in yeast. (*A*) Schematic representation of RIC_{2C}. UV-cross-linked and nonirradiated negative controls were subjected to a first round of 2C. Any residual DNA in the eluates was digested by DNase I, and the RNA and RNA–protein adducts were repurified by a second 2C extraction. Eluates from the second round were RNase I–treated and proteins were subjected to TMT labeling and mass spectrometry analysis. (*B*) Volcano plot displaying $\log_2$ fold change of protein abundance versus −log10 *P*-value after RIC_{2C} of CL and NoCL samples. Gray dots represent proteins displaying no statistically significant difference. Orange dots represent proteins statistically enriched (logFC ≥ 1 and *P*-value ≤ 0.05) in CL over NoCL samples. Glycolytic enzymes statistically enriched in the CL fraction are highlighted with black circles. (*C*) Top 10 significantly ($P_{adjusted} < 0.05$) enriched GO molecular functions, cellular components and biological processes terms of RBPs identified by RIC_{2C} compared to the identified background. (*D*) Venn diagram showing the overlap between the RBPs detected by RIC_{2C}, TRAPP (Shchepachev et al. 2019) and a compendium of other RNA interactome capture experiments in yeast (Scherrer et al. 2010; Tsvetanova et al. 2010; Mitchell et al. 2013; Ray et al. 2013; Kramer et al. 2014; Beckmann et al. 2015; Matia-Gonzalez et al. 2015; Brannan et al. 2016; Shchepachev et al. 2019). (*E*) Analysis of the RBPs detected after RIC_{2C} in yeast. RBPs were categorized according to experimental evidence described in literature ("known"), their detection on RIC experiments (RIC) or content of RNA binding domains (RBD). Novel RBPs detected by RIC_{2C} unrelated to previous experimental evidence and not detected on any RIC experiment were categorized as "unknown." (*F*) Validation of two RBPs by 2C-western blot. A total of 10 µg of 2C RNA from CL and NoCL samples were treated or not with RNase I, separated by SDS-PAGE, blotted to a nitrocellulose membrane and probed against Pab1 and GAPDH antibodies.

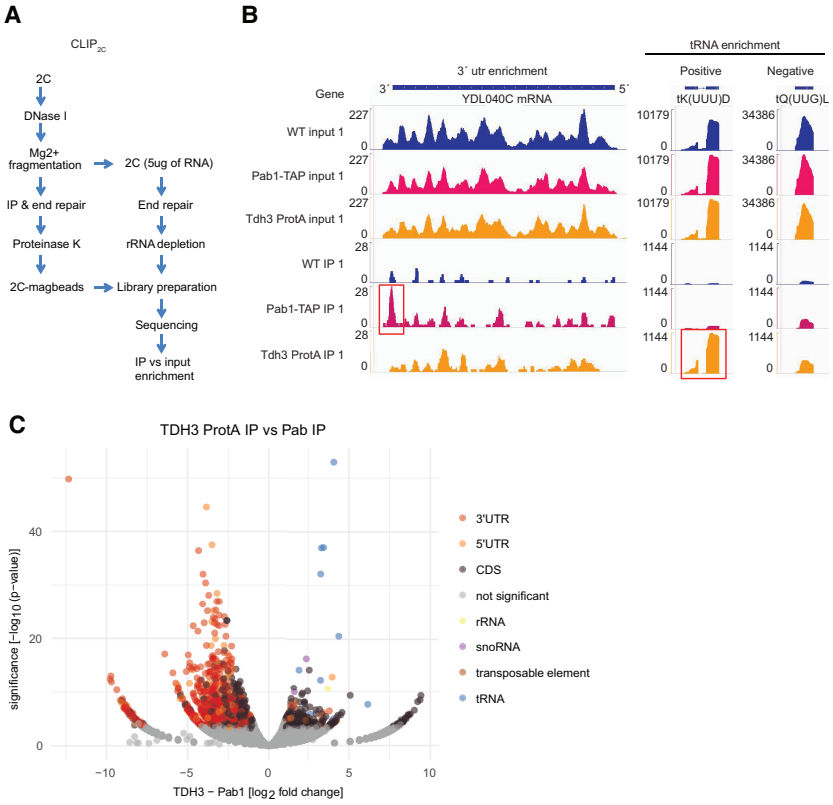

FIGURE 2. $CLIP_{2C}$ identifies several tRNAs as specific GAPDH biding partners. (*A*) Schematic representation of $CLIP_{2C}$ workflow. (*B*) Read coverage along YDL040C, tK(UUU)D, and tQ(UUG)L genes after $CLIP_{2C}$ of Pab1-TAP and Tdh3-Protein A. An untagged WT strain was used as negative control. Scale of the *y*-axis for input and IPs samples were normalized to the highest value. Red boxes highlight statistically significant RNA target regions, the 3′UTR region of YDL040C for Pab1-TAP and tK(UUU)D for Tdh3. The binding of Tdh3 to tK(UUU)D was specific as alternative tRNA genes, like tQ(UUG)L, were not statistically enriched after $CLIP_{2C}$. (*C*) Volcano plot displaying the $\log_2$ fold change in normalized read counts versus $-\log_{10}$ *P*-value after $CLIP_{2C}$ of Tdh3-Protein A and Pab1-TAP. Statistical significance was defined as $\log_2 FC \geq 1$ and *P*-value ≤ 0.05.

samples were used to assess variability in gene expression between the different strains, and sequencing data from the IPs served to detect the GAPDH target RNAs. One thousand two hundred and ninety genes were identified as targets of Pab1 and as expected from a poly(A)-binding RBP, 3′UTR regions were found to be particularly enriched. Three hundred and twenty-six genes, including 299 protein coding mRNAs, were identified as targets of Tdh3. This includes several tRNAs and a subset of mRNAs encoding for proteins of the glycolytic pathway (Fig. 2B; Supplemental Table 2). However, the defined shift of RNA-cross-linked GAPDH by ∼25 kDa suggests that the tRNAs might be preferential targets of GAPDH (Fig. 1F; Supplemental Figs. 2, 3). No enrichment was observed for the WT negative control sample, strongly supporting the specificity of the results. Overall, 12 different tRNAs are significantly enriched in the Tdh3 IPs, while no tRNA was enriched in the IPs of Pab1 (Fig. 2C; Supplemental Table 2). Thus, similarly to the human protein, yeast GAPDH also binds tRNAs in vivo.

$snRIC_{2C}$ yields the yeast proteome of small noncoding RNA-binding proteins

Which other RBPs might preferentially bind to tRNAs or other small noncoding RNAs? We wondered whether 2C could be adapted to address this question, because the binding of small versus longer RNAs to silica matrices is known to be sensitive to the concentration of ethanol in the buffer (Hu et al. 2020). Starting with a 2C total RNA eluate (Fig. 3A, upper panel), we separated RNAs longer (Fig. 3A, middle panel) and shorter (Fig. 3A, lower panel) than 200 nt, respectively, during a second round of differential 2C (see Materials and Methods section for experimental details). Using a bioanalyzer chip optimized to resolve small RNAs, the shorter RNA fraction is found to peak at 66 nt, close to the length of yeast tRNAs (Fig. 3B). While the small RNA fraction shows little if any contamination by longer RNAs (Fig. 3A, bottom panel), the long RNA fraction still includes noticeable amounts of small RNAs (Fig. 3A, middle panel). When 10× long (15

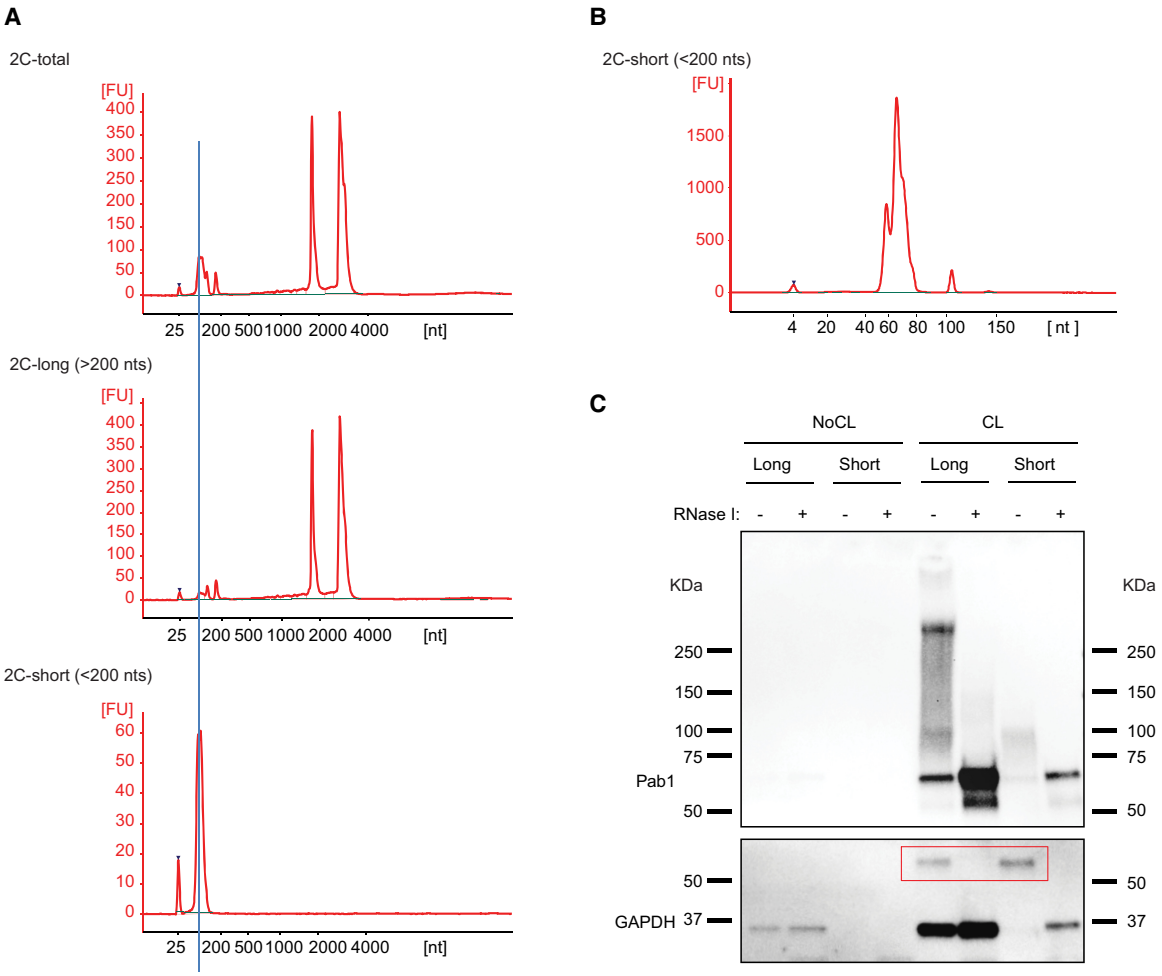

FIGURE 3. GAPDH is enriched in a fraction of short 2C-RNAs. (*A*) Partition of 2C RNA based on RNA length. 2C RNA from a first extraction was subjected to a second round of 2C under conditions that retain total RNA (*upper* bioanalyzer electropherogram), RNA molecules longer than 200 nt (*middle* electropherogram) or RNA molecules shorter than 200 nt (*lower* electropherogram). (*B*) Bioanalyzer electropherogram of 2C short RNA loaded on a short RNA chip. (*C*) 2C RNA from the long and short fractions from CL and NoCL samples were assayed by 2C-western blot and probed against Pab1 and GAPDH antibodies. RNA loaded for the long and short fractions was 15 and 1.4 µg, respectively. GAPDH–RNA complexes are highlighted in the red box.

µg) and 1× short (1.4 µg) RNA were compared by western blotting for GAPDH following 2C, the signal of shifted GAPDH–RNA complexes from short RNA exceeds that from long RNA, reflecting a strong enrichment of cross-linked GAPDH in the 2C short RNA fraction (Fig. 3C). As expected, cross-linked Pab1 is strongly enriched in the long RNA fraction, supporting the specificity of the size separation process.

Based on the successful determination of the total RNA-binding proteome by RIC_{2C} and the excellent separation between small and long RNAs using 2C, we felt encouraged to apply 2C for the determination of the first proteome-wide data set of proteins that bind to small noncoding RNAs by $snRIC_{2C}$ (Fig. 4A). In essence, UV-cross-linked and non-cross-linked samples were subjected to a first round of 2C and eluates were treated with DNase I, as in RIC_{2C}. Each sample was then split into two equal aliquots for a second round of 2C. One aliquot followed the RIC_{2C} protocol and underwent a second round of 2C for elution of total RNA; the second aliquot was used for differential 2C to isolate the small RNA fraction. Cross-linked proteins copurified with the 2C total and small RNA fractions from the second round were then furnished with tandem mass tags (TMT) and analyzed by mass spectrometry. The raw TMT signals showed high reproducibility between experimental repeats and a clear enrichment of the total and small RNA-cross-linked samples over their respective non-cross-link controls (Supplemental Fig. 4A,B).

Around 1000 RBPs were identified in the total RNA samples with an overlap of over 75% with the original RIC_{2C} experiment (Supplemental Fig. 4C), reflecting the reproducibility of the method. $snRIC_{2C}$ identified 311 proteins that bind to purified small RNAs (Fig. 4B,C; Supplemental Table 3), including 52 RBPs that were not previously

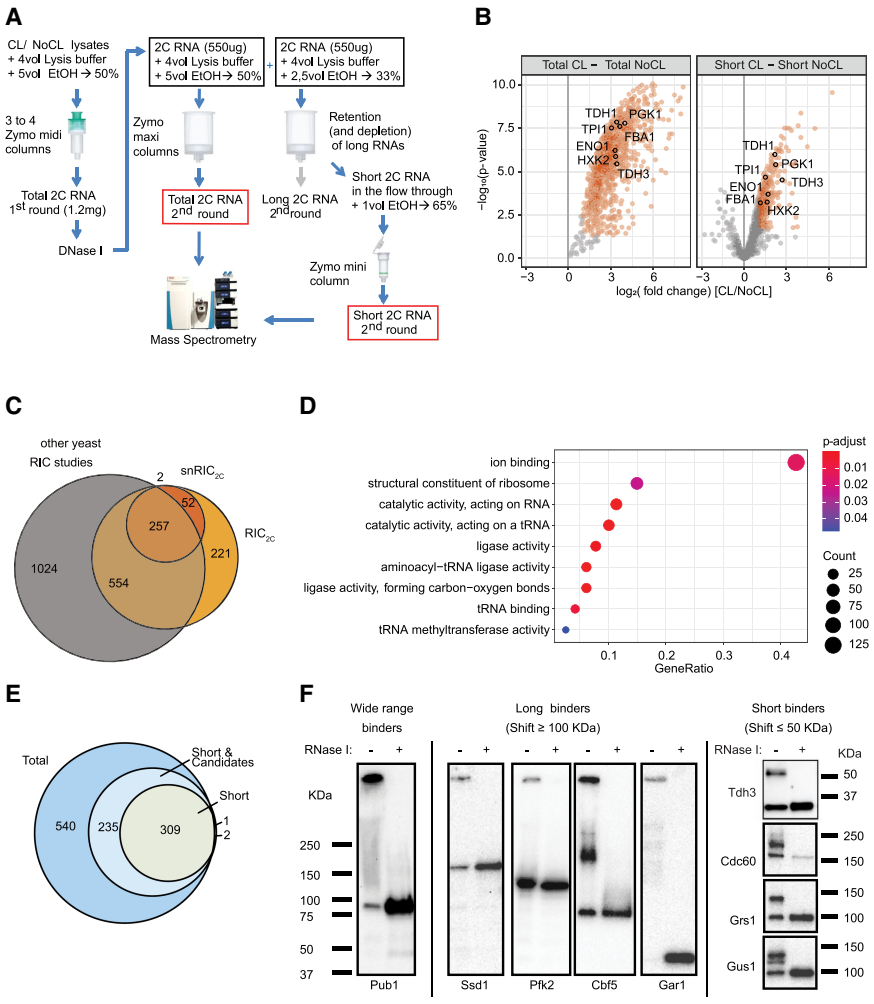

FIGURE 4. snRIC$_{2C}$ identified 311 short RNA binding proteins in yeasts. (*A*) Schematic representation of snRIC$_{2C}$ workflow. (*B*) Volcano plot displaying $\log_2$ fold change of protein abundance versus $-\log_{10}$ *P*-value for total (*left* panel) and short (*right* panel) 2C-RNA, respectively. Orange dots represent statistically significantly enriched proteins in CL versus NoCL samples. Glycolytic enzymes statistically enriched in the CL RNA fractions are highlighted. (*C*) Comparison of RBPs detected in the short RNA fraction versus the 2C total RNA fraction or any other yeast RIC experiment. (*D*) Top 10 significantly enriched GO molecular functions terms of short RNA binding proteins identified by snRIC$_{2C}$ compared to RIC$_{2C}$. (*E*) Venn diagram classifying the RBPs identified in the snRIC$_{2C}$ experiment. Proteins statistically enriched (logFC higher than 1 and *P*-value lower than 0.05) in the total RNA fraction and not enriched in the short RNA one, were considered long RNA binders. Proteins statistically enriched in the short RNA fraction were considered short RNA binders. Proteins statistically enriched in the total RNA fraction and candidate hits in the short RNA fraction (logFC between 0.5 and 1 and *P*-value lower than 0.05) were considered wide range RNA binders (light blue circle). (*F*) Validation of the classification of RBPs based on the length of RNA target molecules by 2C-western blot. TAP-tagged and an untagged WT strain were UV cross-linked, and 1 mg of lysate was subjected to a 2C extraction for total RNA. TAP-tagged strains were probed with a PAP antibody for Protein A detection. The untagged WT strain was probed with a GAPDH antibody. Pub1-TAP was tested as a wide range RBP. Ssd1-TAP, Pfk2-TAP, Cbf5-TAP, and Gar1-TAP were tested as long RNA binders. GAPDH, in the untagged WT strain, Cdc60-TAP, Grs1-TAP, and Gus1-TAP were tested as short RNA binders.

annotated as such in yeast (Fig. 4C). Subsequent GO-term analysis of these proteins showed a strong enrichment for terms related to tRNA metabolism (Fig. 4D), as expected, supporting the validity of snRIC$_{2C}$.

While the differential 2C elution yields quite pure small RNA fractions without noticeable long RNA contamination, the converse does not apply to the long RNA fraction (Fig. 3A). Therefore, we only considered the cross-linked proteomes associated with total and small RNA for comparative analyses (Fig. 4E). Together with the 311 highly enriched proteins in the short RNA fraction, we found 235 additional proteins that fell slightly below the statistical threshold for significance in snRIC$_{2C}$ ($\log_2$FC ≥ 1 and *P*-value ≤ 0.05) but were strongly enriched in RIC$_{2C}$. We suggest that these RBPs likely bind long and small RNAs ("wide range RBPs"). Finally, 540 RBPs were detected by RIC$_{2C}$ but undetected in snRIC$_{2C}$ samples and, therefore, are considered as preferential long RNA binders (Fig. 4E).

To validate these data, we used different TAP-tagged strains and examined UV-cross-linked and non-cross-

linked samples of these by western blot following 2C. In addition to GAPDH (Tdh3), three tRNA synthetases identified as small RNA binders were examined: Cdc60, Grs1, and Gus1. As observed before with GAPDH, all four RBPs show a sharp, RNase-sensitive additional band migrating <50 kDa more slowly than the native proteins before RNase treatment (Fig. 4F). In contrast, the "wide range binder" Pub1 and the long RNA binders Ssd1, Pfk2, Cbf5, and Gar1 all show different patterns with RNase-sensitive smears and/or additional bands migrating >100 kDa more slowly or being retained in the wells of the gel. These results support the assignment of small noncoding RNA binders by snRIC$_{2C}$, and confirm that the shifts observed in 2C immunoblots correlate well with the lengths and homo-/heterogeneity of the bound RNAs.

Analysis of small noncoding RBPs reveals enrichment of glycolytic and TCA cycle enzymes

Classification of the snRBPs shows that 41% of the 311 RBPs are enzymes, including 45 metabolic enzymes (Fig. 5A). Among the metabolic enzymes, processes related to tRNA metabolism and carbohydrate derivative metabolic processes are strongly enriched (Fig. 5B). Interestingly, 10 glycolytic enzymes (Hxk2, Fba1, Tdh1-3, Tpi1, Pgk1, Gpm1, and Eno1-2) and five enzymes of the TCA cycle (Aco1, Idh1, Mdh1, Lsc1, and Lpd1) were identified as snRBPs (Figs. 4B, 5C), and aminoacyl-tRNA biosynthesis and carbon metabolism are the two significantly enriched pathways among the snRIC$_{2C}$ hits (Fig. 5D). To confirm this striking enrichment, we tested several further TAP-tagged strains in 2C-western blot experiments, using an untagged WT strain as a negative control (Supplemental Fig. 5). These experiments confirm that the glycolytic enzymes Tdh3, Fba1, Pgk1, Hxk2, Gpm1, Tpi1, and Eno1 all show the defined, RNase-sensitive additional band less than 50 KDa larger than the expected size of the respective proteins (Fig. 5E). We conclude that several yeast glycolytic enzymes bind small noncoding RNAs in addition to their well-known roles in central carbon metabolism.

Small noncoding RNA binding of GAPDH is carbon source–dependent and regulated by Maf1

We wondered whether the binding of glycolytic enzymes to small noncoding RNAs is constitutive or subject to biological regulation. A growing body of evidence links nutrient availability with the regulation of RNA polymerase III activity by its universal repressor Maf1 (Morawiec et al. 2013; Graczyk et al. 2018; Willis 2018). Under favorable growth conditions like fermentation, Maf1 is repressed, allowing high Pol III activity and tRNA transcription. Conversely, growth under respiratory conditions results in Maf1 activation, which represses Pol III activity and tRNA synthesis (Cieśla et al. 2007; Morawiec et al. 2013; Graczyk et al. 2018; Willis 2018). Therefore, we tested whether the tRNA binding activity of GAPDH responds to changes of the carbon source in the growth media and is affected by Maf1. When WT and Maf1 KO cells were grown in glucose, a fermentative carbon source, or glycerol and ethanol, which can only be respired, we observed tRNA engagement of GAPDH only under fermentative conditions (Fig. 6). Under these conditions, RNA binding is unaffected by Maf1 deletion. However, deletion of Maf1 strongly induces the binding of GAPDH to tRNA under respiratory conditions, in contrast to mitochondrial ATP1, another enzyme of energy metabolism that we identified as an RBP by RIC$_{2C}$ (Supplemental Table 1) and that we used as a specificity control. These results uncover a connection between tRNA binding of glycolytic enzymes, the activity of the glycolytic pathway that is influenced by the prevalent carbon source and Pol III activity.

DISCUSSION

We previously showed that commercially available silica columns for the purification for total cellular RNA can also be used to select for RBPs that are covalently cross-linked to these RNAs, offering a simple method (called complex capture [2C]) to test the RNA-binding activity of proteins by simple immunoblotting of 2C eluates (Asencio et al. 2018). Realizing that the 2C principle can also be used to determine the total RNA-binding proteomes of cells if eluates are analyzed by sensitive mass spectrometry, we applied this method to the yeast *Saccharomyces cerevisiae*. Our unexpected biological observations drove further methodological advances, and this work hence reports both the development of enabling methods and new biological insights on the interaction of glycolytic enzymes with small noncoding RNAs in yeast.

Methodological advances

RIC$_{2C}$

Based on our earlier work, 2C could be readily applied to the determination of the proteome that binds to any class of cellular RNAs. For yeast, we found a total number of 983 RBPs, which is in keeping with other reports both in terms of the number and the identity of the RBPs. This result both validates RIC$_{2C}$ methodologically and suggests that at least under standard growth conditions the number of yeast RBPs appears to approximate saturation, since we identified only a modest number of 174 RBPs that were not detected previously. RIC$_{2C}$ provides advantages compared to alternative methods. It does not require in vivo labeling of RNA with nucleotide analogs, like CARIC (Huang et al. 2018). RIC$_{2C}$ is simple, easily scalable and does not require the challenging isolation of RBPs from the interphase between two solvents, as in OOPS, XRNAX, and

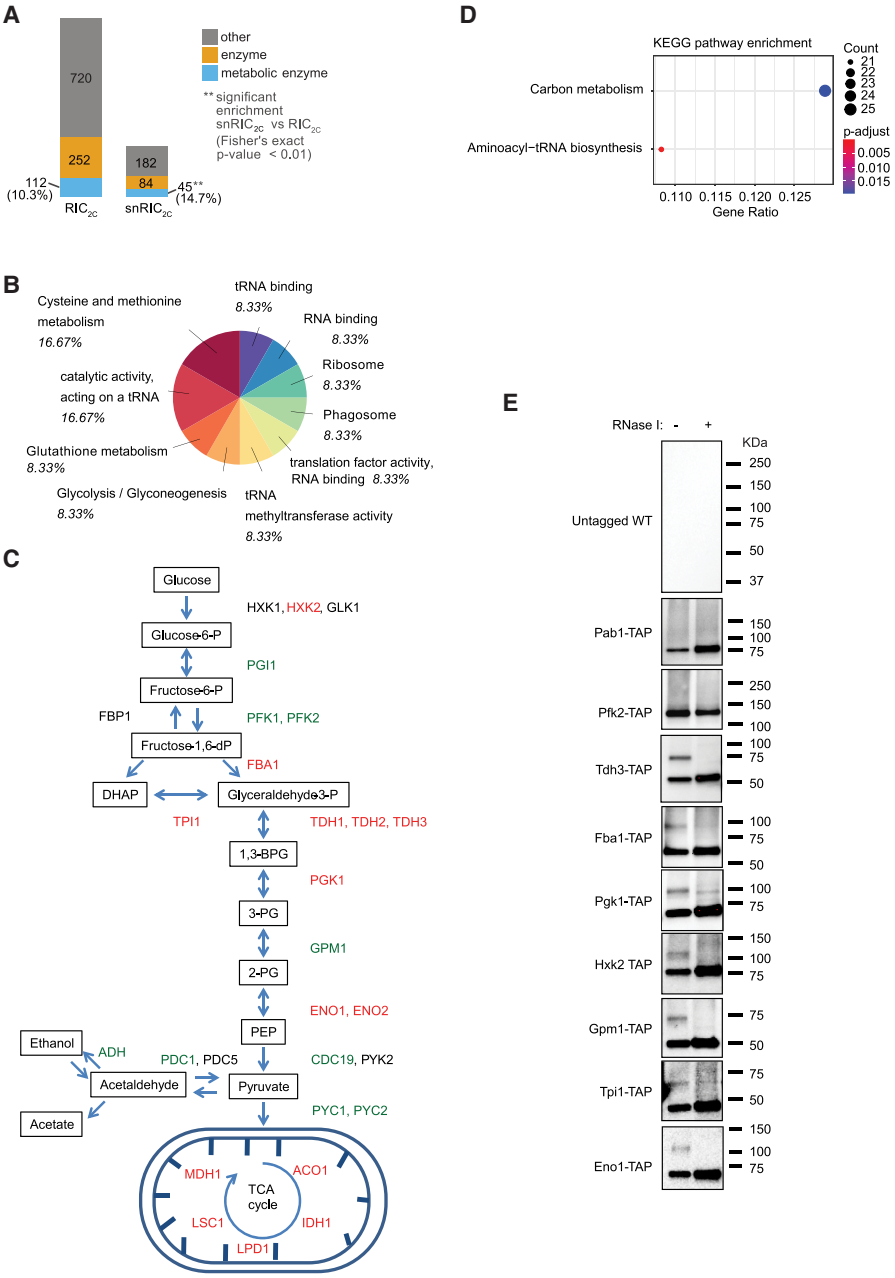

FIGURE 5. Glycolytic pathway is enriched in short RNA binding proteins. (*A*) Analysis of proteins found in snRIC$_{2C}$ experiment. (*B*) Go-term molecular function and Interpro domain analysis of the proteins enriched in the CL short fraction in snRIC$_{2C}$ experiment. (*C*) Schematic representation of glycolysis and TCA cycle pathways. Proteins highlighted in green were identified as long or wide range RBPs, and proteins highlighted in red were found to bind short RNAs in snRIC$_{2C}$. (*D*) Analysis of KEGG enriched pathways after snRIC$_{2C}$. Aminoacyl-tRNA biosynthesis and carbon metabolism pathways were found to be statistically enriched from the proteins detected in the short RNA fraction in snRIC$_{2C}$ experiment. (*E*) Validation of glycolytic and TCA enzymes as short RBPs by 2C-WB. TAP-tagged strains and an untagged WT strain were UV-cross-linked and 1 mg of lysate was used in a round of total 2C-RNA extraction. Blots were probed against PAP antibody. The untagged WT strain was tested as a negative control for the western blot. Pab1-TAP and Pfk2-TAP were used as controls as wide range and long RNA binders, respectively. Tdh3-TAP, Fba1-TAP, Pgk1-TAP, Hxk2-TAP, Gpm1-TAP, Tpi1-TAP, and Eno1-TAP were tested as short RNA binders.

PTex (Queiroz et al. 2019; Trendel et al. 2019; Urdaneta et al. 2019). Moreover, organic phase separation methods like OOPS can underrepresent RBPs bound to small RNAs (Queiroz et al. 2019). RIC$_{2C}$ conceptually corresponds to the recently published TRAPP protocol (Shchepachev et al. 2019), where silica powder is used as the starting material for the enrichment of total RNA-binding proteins. RIC$_{2C}$ does not require extensive washing and preparation steps for the purification columns prior to the application of samples, because it uses columns and buffers contained

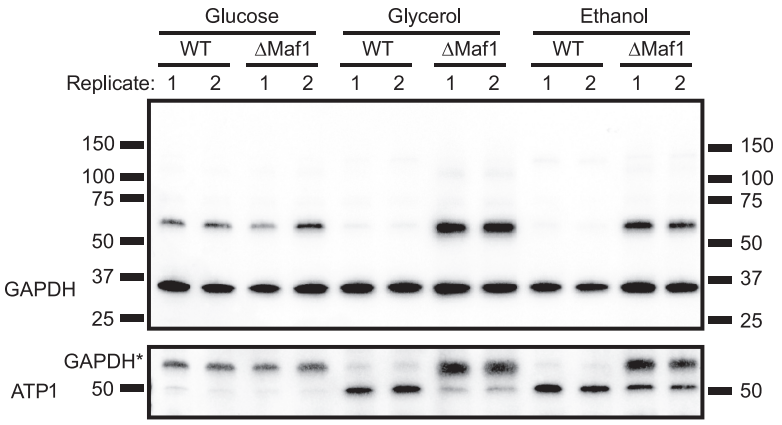

FIGURE 6. Engagement of GAPDH to tRNAs is carbon source–dependent and regulated by the RNA polymerase III universal repressor Maf1. WT and ΔMaf1 strains were grown in glucose, glycerol and ethanol and UV-cross-linked. Total 2C RNA extractions were performed from two different biological replicates and 20 µg of RNAs were tested on 2C-western blots against GAPDH and ATP1 antibodies. GAPDH* represents residual GAPDH signal after stripping and reprobing the membrane.

in commercially available RNA extraction kits. Therefore, it is a simple and straightforward method that can be applied to a wide range of biological materials, both eukaryotic and prokaryotic in origin. Because different column sizes are commercially available, it is simple to scale RIC_{2C} to the experimental needs.

$CLIP_{2C}$

UV-cross-linking followed by immunoprecipitation and library preparation from the coprecipitated RNAs is commonly used to determine the RNAs bound to an RBP of interest (Darnell 2010; Van Nostrand et al. 2016; Lee and Ule 2018; Ule et al. 2018). While CLIP protocols typically perform well when studying canonical, high affinity RBPs such as for example, RNA processing factors, they can fall short with noncanonical, lower affinity RBPs, where often only a minor fraction of the protein is RNA-bound which can give rise to a high nonspecific background. $CLIP_{2C}$ offers a simple enrichment step for the RNA-bound fraction of an RBP of interest (Fig. 2A; Supplemental Fig. S2) before immunoprecipitation. The resulting RNA-loaded RBP subsequently represents an ideal substrate for library generation and sequencing, because contaminant proteins in the immunoprecipitation are reduced. Nonetheless, 2C requires protein denaturing conditions, which potentially compromises the subsequent immunoprecipitation step if the antibody used recognizes a natively folded epitope. Therefore, antigen-antibody pairs should be pre-evaluated for their compatibility with denatured/renatured proteins. We also show that proteins bearing protein-A tags can be efficiently pulled-down from 2C eluates, subsequently yielding excellent sequencing results. We used $CLIP_{2C}$ to demonstrate for the first time that yeast GAPDH binds tRNAs in vivo, supporting the evolutionary conservation of the GAPDH–tRNA interaction previously reported for human GAPDH (Singh and Green 1993).

$snRIC_{2C}$

Unlike other methods for the capture of RNA-binding proteomes, the silica matrix-based approach allows robust and reproducible separation of small (<200 nt) from longer RNAs. We show here that based on this principle $snRIC_{2C}$ can be used to determine the collective of RBPs that binds to small noncoding RNAs. As discussed below, this collective displays interesting distinctions from the total RNA-bound proteome as a whole. To the best of our knowledge, $snRIC_{2C}$ represents the first method for the systematic isolation of RBPs based on the lengths of their target RNAs. $snRIC_{2C}$ may also be of particular interest for the field of bacterial small RNA metabolism, as small noncoding RNAs are highly recognized for their critical regulatory roles in bacteria (Jørgensen et al. 2020; Quendera et al. 2020; Ponath et al. 2022), but methods to identify and study their associated RBPs are still needed.

New biological data sets and insights

Identification of the snRBPs from yeast

Using $snRIC_{2C}$, we identified ~300 yeast proteins that are highly enriched for binding to small noncoding RNAs, snRBPs (Fig. 5). Since small noncoding RNAs exert numerous regulatory functions, it is important to reveal the snRBPs with which they preferentially interact. Unsurprisingly, the snRBPs include many proteins known for their roles in tRNA metabolism and function. But it is quite unexpected to find so many glycolytic and TCA cycle enzymes among the snRBPs (Figs. 4B, 5C). Earlier work connected yeast glycolytic enzymes with tRNAs. For instance, enolase has been found to bind tRNAs in vivo (Shchepachev et al. 2019) and has been proposed to participate in the import of tRNA to mitochondria in yeast (Entelis et al. 2006). Interestingly, while enolase was originally considered to directly contribute to the import of tRNA into mitochondria, later publications favor the view that enolase accompanies other proteins participating in this process (Baleva et al. 2017). Our results broadly implicate glycolytic enzymes and TCA cycle enzymes in the binding of small noncoding RNAs. At least for GAPDH, these largely appear to be tRNAs (Fig. 2B,C). These

observations raise the question of what the function(s) of these RNA–protein interactions may be. As exemplified above and by other examples, the enzymes may moonlight in critical aspects of small noncoding RNA biology. Alternatively, the RNAs may riboregulate the enzymes that they bind to. Riboregulation has recently been shown for human enolase 1 (Huppertz et al. 2022), the human small noncoding vtRNA1-1 has been identified to regulate mammalian autophagy by binding to the receptor protein p62 (Horos et al. 2019), and RNA has been found to promote phase separation of glycolytic enzymes into G bodies under hypoxic conditions (Fuller et al. 2020)

With ~300 yeast snRBPs having been identified and the application of snRIC$_{2C}$ to other organisms, we expect further insights into the biological functions of small noncoding RNAs.

A carbon source–dependent interaction between glycolysis and RNA polymerase III activity

Cells dedicate profound resources to protein production, not only involving translation itself, but also including the transcription, maturation and amino-acylation of tRNAs. Therefore, cells must monitor nutrient availability and modulate protein and tRNA synthesis accordingly. The activity of the tRNA-synthesizing Pol III is inhibited under nutrient limiting conditions by the repressor protein Maf1 (Upadhya et al. 2002). Here, we show that the binding of tRNAs to GAPDH is affected by Maf1 activity: increased tRNA levels in the Maf1 KO strain grown under respiratory conditions (Cieśla et al. 2007) are accompanied by increased tRNA–GAPDH engagement. Interestingly, earlier work identified regulatory interactions between carbon metabolism enzymes and Pol III activity (Cieśla et al. 2007; Morawiec et al. 2013; Szatkowska et al. 2019), but fell short of noticing the direct and carbon source–dependent interaction of glycolytic enzymes with Pol III transcripts. Our findings suggest a connection between nutrient availability, energy metabolism and Pol III activity, and more research will serve to analyze the functional role of these interactions in detail.

MATERIALS AND METHODS

S. cerevisiae strains and manipulations

Standard methods were used for yeast culture and manipulation (Amberg et al. 2005). Yeast strains, genotype and origin are summarized in Table 1.

Yeast culture, cross-linking, lysate preparation, 2C method, and 2C-western blot

Yeast culture, UV cross-linking, cell lysis, 2C method and 2C-western blot experiments were done as previously described (Asencio et al. 2018). The following antibodies were used in western blot experiments: Anti-Pab1 1:4000 (Abcam, #ab189635), Anti-GAPDH 1:4000, a polyclonal antibody that detects all three Tdh (Tdh1, Tdh2, and Tdh3) yeast GAPDH isoforms (Sigma-Aldrich #G9545 [33]), Anti-histone H3 HRP 1:1000 (Abcam, #ab21054), Anti-Hexokinase 1:10000 (Bio-Rad, #4959-9988), Anti-Tpi 1:4000 (Proteintech, #10713-1-AP), Anti-tubulin 1:4000 (Abcam,

TABLE 1. *Saccharomyces cerevisiae* strains used in this study

Strain	Genotype	Source
WT BY4741	MATa *his3Δ1 leu2Δ0 met15Δ0 ura3Δ0*	Horizon Discovery Ltd.
ΔMaf1	MATa *his3Δ1 leu2Δ0 met15Δ0 ura3Δ0 maf1Δ*	Horizon Discovery Ltd.
Cbf5-TAP	MATa *his3Δ1 leu2Δ0 met15Δ0 ura3Δ0 CBF5-TAP::His3Mx6*	Horizon Discovery Ltd.
Cdc60-TAP	MATa *his3Δ1 leu2Δ0 met15Δ0 ura3Δ0 CDC60-TAP::His3Mx6*	Horizon Discovery Ltd.
Eno1-TAP	MATa *his3Δ1 leu2Δ0 met15Δ0 ura3Δ0 ENO1-TAP::His3Mx6*	Horizon Discovery Ltd.
Fba1-TAP	MATa *his3Δ1 leu2Δ0 met15Δ0 ura3Δ0 FBA1-TAP::His3Mx6*	Horizon Discovery Ltd.
Gar1-TAP	MATa *his3Δ1 leu2Δ0 met15Δ0 ura3Δ0 GAR1-TAP::His3Mx6*	Horizon Discovery Ltd.
Gpm1-TAP	MATa *his3Δ1 leu2Δ0 met15Δ0 ura3Δ0 GPM1-TAP::His3Mx6*	Horizon Discovery Ltd.
Grs1-TAP	MATa *his3Δ1 leu2Δ0 met15Δ0 ura3Δ0 GRS1-TAP::His3Mx6*	Horizon Discovery Ltd.
Gus1-TAP	MATa *his3Δ1 leu2Δ0 met15Δ0 ura3Δ0 GUS1-TAP::His3Mx6*	Horizon Discovery Ltd.
Hxk2-TAP	MATa *his3Δ1 leu2Δ0 met15Δ0 ura3Δ0 HXK2-TAP::His3Mx6*	Horizon Discovery Ltd.
Pab1-TAP	MATa *his3Δ1 leu2Δ0 met15Δ0 ura3Δ0 PAB1-TAP::His3Mx6*	Horizon Discovery Ltd.
Pfk2-TAP	MATa *his3Δ1 leu2Δ0 met15Δ0 ura3Δ0 PFK2-TAP::His3Mx6*	Horizon Discovery Ltd.
Pgk1-TAP	MATa *his3Δ1 leu2Δ0 met15Δ0 ura3Δ0 PGK1-TAP::His3Mx6*	Horizon Discovery Ltd.
Pub1-TAP	MATa *his3Δ1 leu2Δ0 met15Δ0 ura3Δ0 PUB1-TAP::His3Mx6*	Horizon Discovery Ltd.
Ssd1-TAP	MATa *his3Δ1 leu2Δ0 met15Δ0 ura3Δ0 SSD1-TAP::His3Mx6*	Horizon Discovery Ltd.
Tdh3 Protein A	MATa *his3Δ1 leu2Δ0 met15Δ0 ura3Δ0 TDH3-ProtA::His3Mx6*	(Asencio et al. 2018)
Tdh3-TAP	MATa *his3Δ1 leu2Δ0 met15Δ0 ura3Δ0 TDH3-TAP::His3Mx6*	Horizon Discovery Ltd.
Tpi1-TAP	MATa *his3Δ1 leu2Δ0 met15Δ0 ura3Δ0 TPI1-TAP::His3Mx6*	Horizon Discovery Ltd.

#ab6160), and Anti-PFK antibody 1:4000 (Heinisch 1986). Peroxidase anti-peroxidase (PAP) antibody 1:10,000 was used to detect all TAP and Protein A tagged proteins (Sigma-Aldrich # P1291); Anti-ATP5b 1:1000 (Proteintech, #17247-1-AP) was used to detect the yeast ortholog protein ATP1.

Up- and downscaling the 2C method

In our original description of the 2C method, we used Zymo-Spin V-E (#C1024; Zymo Research) columns which are included in Zymo Research RNA Extraction Midi Kits or can be purchased separately. However, the 2C method can be up- or downscaled depending on the required amount of 2C RNA and/or the available input material. We have successfully tested Zymo Research micro (Zymo-Spin IC, #C1004), mini (Zymo-Spin IIICG, #C1006), and maxi (Zymo-Spin VI, #C1013) columns. Alternatively, several columns can be used in parallel to process different aliquots of the same lysate simultaneously.

2C total RNA interactome capture (RIC_{2C})

WT yeast cells were grown, UV-cross-linked and lysed as described above. Nonirradiated cells were cultured and processed in parallel throughout the experiment as negative controls. Three biological replicates were included in the experiment. A first round of 2C extraction was performed from 1 mg of protein lysate with Zymo-Spin V-E columns, and 2C-RNA was later eluted with 300 µL of nuclease-free water. Although in our hands, the DNA contamination after a 2C extraction from a yeast lysate is below 2%, we nevertheless treated the eluates with 20 U of DNase I (AM2224, Ambion) at 37°C for 30 min to minimize the chances of detecting DNA binding proteins after mass spectrometry analysis. A second round of 2C was performed to eliminate the DNase I enzyme and any contaminant DNA binding protein. For this, four volumes of RNA lysis buffer were added to the DNase I–treated samples. Samples were mixed, five volumes of ethanol were added, and after mixing, the samples were added to a second Zymo-Spin V-E column. Second round 2C-RNA was eluted with 300 µL of nuclease-free water. An amount of 100 µg of 2C RNA eluates were RNase I–treated and processed for TMT labeling. Briefly, cysteines were reduced with dithiothreitol at 56°C for 30 min (10 mM in 50 mM HEPES, pH 8.5) and further alkylated with 2-chloroacetamide at room temperature in the dark for another 30 min (20 mM in 50 mM HEPES, pH 8.5). Samples were processed using the SP3 protocol (Hughes et al. 2014) and on-bead digested with trypsin (sequencing grade, Promega), which was added in an enzyme to protein ratio 1:50 for overnight digestion at 37°C. Peptides were modified with TMTsixplex (Dayon et al. 2008) Isobaric Label Reagent (Thermo Fisher) following manufacturer's instructions. For sample clean up, an OASIS HLB µElution Plate (Waters) was used. Offline high pH reverse phase fractionation was performed on an Agilent 1200 Infinity high-performance liquid chromatography system, equipped with a Gemini C18 column (3 µm, 110 Å, 100 × 1.0 mm, Phenomenex), resulting in five fractions.

For mass spectrometry data acquisition, an UltiMate 3000 RSLC nano LC system (Dionex) fitted with a trapping cartridge (µ-Precolumn C18 PepMap 100, 5 µm, 300 µm i.d. × 5 mm, 100 Å) and an analytical column (nanoEase M/Z HSS T3 column 75 µm × 250 mm C18, 1.8 µm, 100 Å, Waters) was used. Trapping was carried out with a constant flow of trapping solution (0.05% trifluoroacetic acid in water) at 30 µL/min onto the trapping column for 6 min. Subsequently, peptides were eluted via the analytical column running solvent A (0.1% formic acid in water) with a constant flow of 0.3 µL/min, with an increasing percentage of solvent B (0.1% formic acid in acetonitrile) from 2% to 4% in 4 min, then 4% to 8% in 2 min, from 8% to 28% for a further 66 min, in another 10 min from 28% to 40%, followed by an increase of B from 40%–80% for 3 min and a reequilibration back to 2% B for 5 min. The outlet of the analytical column was coupled directly to a QExactive plus Mass Spectrometer (Thermo) using the Nanospray Flex ion source in positive ion mode.

Mass spectrometry analysis for RIC_{2C} and $snRIC_{2C}$ experiments

IsobarQuant (Franken et al. 2015) and Mascot (v2.2.07) were chosen for data processing. A Uniprot *Saccharomyces cerevisiae* proteome database (UP000002311) containing common contaminants and reversed sequences was used. The search parameters were the following: carbamidomethyl (C) and TMT10 (K) (fixed modification), acetyl (N-term), oxidation (M), and TMT10 (N-term) (variable modifications). A mass error tolerance of 10 ppm was set for the full scan (MS1) and for MS/MS (MS2) spectra of 0.02 KDa. Trypsin was selected as protease with an allowance of a maximum of two missed cleavages. A minimum peptide length of seven amino acids and at least two unique peptides were required for individual protein identification. The false discovery rate on peptide and protein level was set to 0.01.

$CLIP_{2C}$

Pab1-TAP, Tdh3-Protein A and a WT untagged strain were grown in YPD, UV cross-linked and lysed as described above. A first round of 2C was performed from 1 mg of protein lysate, and 100 µg of the obtained 2C-RNA were DNase I–treated for 30 min at 37°C. After DNase I treatment, RNA samples were diluted with RNA fragmentation buffer to a final concentration of 20 mM Tris-HCl pH 7.5, 1% SDS and 30 mM $MgCl_2$. RNA was fragmented by incubating the samples for 15 min at 95°C. Fragmentation was stopped by adding EDTA to a final concentration of 30 mM, quickly cooling down the samples on ice and later kept at room temperature. Samples were brought to 2 mL with buffer B (25 mM Tris-HCl 7.5 mM; 140 mM NaCl, 1.8 mM $MgCl_2$; 0.5 mM DTT and 0.1% NP-40), and 50 and 100 µL were saved for IP validation and input sequencing, respectively. To the remaining volume, 100 µL of prewashed Dynabeads Pan mouse IgG (#11041, Thermo) were added per sample and were incubated at 4°C for 2 h with gentle rotation. Samples were washed once with buffer B, three times with wash buffer (25 mM Tris-HCl 7.5 mM; 1 M NaCl, 1.8 mM $MgCl_2$; 0.5 mM DTT and 0.1% NP-40), and one time with buffer B. After the washing steps the beads were magnetically pelleted, the supernatant was discarded, and the beads were resuspended in 20 mM Tris-HCl pH 7.5. While on the beads, samples were end-repaired by the T4 PNK enzyme (#M0201L, NEB) following manufacturer instructions. After end-repairing, beads were resuspended in 50 µL of proteinase buffer plus 5 µL of proteinase K (#3115828001, Roche), and the samples were

incubated for 1 h at 37°C with gentle rotation. The RNA from the IPs was purified by adding to the beads 200 µL of RNA lysis buffer. Beads were magnetically pelleted and the supernatants were transferred to new tubes. A total of 250 µL of ethanol and 25 µL of Magbeads (#D4100, Zymo Research) were added per sample. Samples were mixed and incubated for 15 min at room temperature with gentle rotation. Beads were magnetically pelleted and washed sequentially with MagBead DNA/RNA Wash1 buffer (#R2130-1, Zymo Research) and MagBead DNA/RNA Wash 2 buffer (#R2130-2, Zymo Research). After magnetically pelleted, beads were resuspended in 30 µL of H_2O. Samples were incubated at 37°C for 15 min, and after magnetically pelleting the beads, the eluted RNA was finally transferred to a new tube.

The saved 100 µL of fragmented 2C-RNA for the inputs were processed in parallel during the 2 h incubation period of the immunoprecipitation. Samples were processed for a second 2C extraction using a Zymo-Spin IC micro column (#C1004, Zymo Research) and 3 µg of the resulting RNA was end-repaired, in a final volume of 50 µL, by the T4 PNK enzyme (#M0201L, NEB) following manufacturer instructions. To eliminate the T4 PNK enzyme and buffers, the RNA was later purified by adding 200 µL of RNA lysis buffer, after mixing and addition of 250 µL of ethanol, 25 µL of Magbeads were added to each sample. Samples were incubated for 15 min at room temperature and gently rotated. Samples were washed with MagBead DNA/RNA wash buffer 1 and 2 as previously described, and RNA was finally eluted in 30 µL of H_2O. After RNA purification, 1 µg of input RNA was subjected to rRNA depletion with the Ribo-Zero Gold Yeast Kit (MRZY1324, Illumina) following manufacturer instructions.

RNA purified from the IPs and ribodepleted RNA from the input samples were processed for library preparation with the Nextflex Small RNA Kit v3 (#NOVA-5132-06, PerkinElmer), following manufacturer instructions. Libraries from three biological replicates of inputs and IPs were pooled together and sequenced on a NextSeq500 (Illumina) instrument on an 80 paired-end run.

Sequencing informatics analysis

Reads were trimmed with Cutadapt (v2.3) and sequencing quality was inspected with FastQC. Novoalign (v3.07.01) was used to map to the yeast genome (sac3). Gene counts were summarized with featureCounts (v1.6.4). DESeq2 (Love et al. 2014) with IHW (Ignatiadis et al. 2016) for multiple hypothesis correction was used to determine significantly enriched RNAs in IP samples vs corresponding input controls (adjusted P-value < 0.5; $\log_2$ fold-change > 1). Transcriptome coverage plots were generated with bamCompare, computeMatrix and plotProfile functions from DeepTools (Ramírez et al. 2014). CSAW (Lun and Smyth 2016) was used to detect significantly enriched regions in the IP samples compared to the input controls.

Fractionation of 2C-RNA in long and short RNA molecules

Four volumes of RNA lysis buffer were added to 100 µg of 2C total RNA extracted following the standard 2C method. After mixing, ethanol was added to a final concentration of 33% (vol/vol). Samples we mixed by gentle vortexing and later added to a Zymo-spin IIICG (#C1006, Zymo Research) column. However, and as described before, the procedure can be up- or down-scaled at will. Under these conditions, the column only retains RNA molecules longer than 200 nt. The flowthrough, containing the short RNA fraction, was transferred to a new tube. Ethanol to a final concentration of 65% (vol/vol) was added; samples were mixed and added to a second silica column (mini or micro column), which will now retain the short RNAs. Both sets of columns, containing separately the long and short RNA fractions were loaded with 400 µL of RNA Prewash buffer and spun at 10,000*g* for 30 sec. The flowthrough was discarded and the columns were washed with 700 µL of RNA wash buffer. Columns were centrifuged at 10,000*g* for 30 sec, the flowthrough discarded and loaded again with 400 µL of RNA wash buffer. Columns were centrifuged at 10,000*g* for 2 min to eliminate any residual ethanol. After the centrifugation, the columns were transferred to new collection tubes and RNA was finally eluted in 50 µL of H20 by centrifugation at 16,000*g* for 1 min. To evaluate the performance of the 2C-RNA fractionation, 1 µL of each sample was assessed with Bioanalyzer RNA nanochips (#5067-1511; Agilent) (Schroeder et al. 2006). In addition, to accurately analyze the 2C-short RNA fraction, 1 µL of the short RNA fraction was also run on a Bioanalyzer Small RNA chip (#5067-1548; Agilent).

2C small noncoding RNA interactome capture ($snRIC_{2C}$)

An untagged WT strain was grown in YPD, UV cross-linked and lysed as previously described. Corresponding nonirradiated cells were processed in parallel as negative controls. A first round of 2C total RNA extractions was performed as previously described, and two vials containing 550 µg of 2C RNA per sample were DNase I–treated at 37°C for 30 min in a final volume of 1 mL. One set of DNase I–treated RNA was used to purify a second round of 2C total RNA, while the second set was used to purify a fraction of 2C short RNA. For the purification of the second round of 2C total RNA, 4 mL of RNA lysis buffer were added to the DNase I–treated RNA, the samples were gently mixed by vortexing, and 5 mL of ethanol to a final concentration of 50% were added. The samples were mixed again and added to a Zymo-Spin VI maxi column (#C1013, Zymo Research) inserted on a 50 mL polypropylene centrifuge tube. Samples were centrifuged at 3000*g* for 5 min and the supernatant was discarded. An amount of 4 mL of RNA prewash buffer was added and the column was centrifuged again at 3000*g* for 5 min. Later, the column was washed twice by centrifugation with 5 mL of RNA wash buffer and finally eluted with 2 mL of H_2O.

For the purification of the second round of 2C short RNA, 2 mL of a 1:1 mixture of RNA lysis buffer and ethanol were added per DNase I–treated sample. The samples were mixed and loaded on a Zymo-spin VI maxi column sitting on a 50 mL Falcon tube. Samples were centrifuged at 3000*g* for 5 min, and 3 mL of ethanol were added to the flowthrough, which contained the short RNA fraction. Samples were mixed and loaded on a Zymo-spin IIICG mini column and centrifuged at 10,000*g* for 30 sec. The flowthrough was discarded and 400 µL of RNA prewash buffer were added to the column and the samples were centrifuged at 10,000*g* for 30 sec. Samples were washed two times sequentially by centrifugation with 700 and 400 µL of wash buffer, respectively. Finally, 100 µL of H_20 were added to the column and the 2C

short RNA fraction was eluted by centrifugation at 16,000*g* for 1 min.

After the second round of 2C, total and short RNA fractions were quantified in Nanodrop 1000 (Thermo Fisher Scientific) and 35 µg of each fraction were RNase I (#AM2295; Ambion) digested in 10 mM Tris-HCl pH 7.5 and 100 mM NaCl for 30 min at 37°C. The resulting RNase I–treated samples were processed for TMTsixplex labeling as described above for the RIC_{2C} experiment with the exception that six fractions per sample were obtained after TMTsixplex labeling. Mass spectrometry data acquisition was done similarly to the RIC_{2C} experiment described above with the exception of the gradient used. In $snRIC_{2C}$, peptides were eluted via the analytical column running solvent A (0.1% formic acid in water, 3% DMSO) with a constant flow of 0.3 µL/min, with an increasing percentage of solvent B (0.1% formic acid in acetonitrile, 3% DMSO) from 2% to 8% in 6 min, then 8% to 28% for a further 42 min, in another 5 min from 28% to 40%, followed by an increase of B from 40%–80% for 4 min and a reequilibration back to 2% B for 4 min. The outlet of the analytical column was coupled directly to an Orbitrap Fusion Lumos Tribrid Mass Spectrometer (Thermo) using the Nanospray Flex ion source in positive ion mode.

Carbon source–dependent tRNA engagement of GAPDH

Precultures of WT and Maf1Δ cells were grown overnight in YPD (2% glucose), YPG (3% glycerol), or YPE (3% ethanol) media. The next day, aliquots were used to start 250 mL cultures at an O.D.600 = 0.1 and grown until mid-log phase (O.D.600 ≈ 0.8). Cells were collected and UV-cross-linked, as described before, with 3 J/cm^2 of UV light at 254 nm. After lysis, a 2C total RNA extraction was performed from 1 mg of protein lysate and the resulting 2C RNA was quantified in nanodrop. An amount of 20 µg of 2C RNA from two biological replicates was run on an SDS-PAGE, blotted to a nitrocellulose membrane and probed with antibodies against GAPDH and human ATP5b, which detects the yeast ortholog ATP1p.

SUPPLEMENTAL MATERIAL

Supplemental material is available for this article.

ACKNOWLEDGMENTS

We thank Dr. T. Sekaran for his support with the data analysis, and current and former members of the Hentze laboratory for their feedback, suggestions and fruitful discussions. We thank the EMBL Genomics, Proteomics and Protein Expression and Purification core facilities for their expert support. We thank C. Girardot for helping with sequencing data deposition. We are grateful to Dr. J. Heinisch for the provision of the anti-Pfk antibody. This work was supported in part by generous funding from the Manfred Lautenschläger Foundation (to M.W.H.).

Received August 10, 2022; accepted November 29, 2022.

REFERENCES

Amberg D, Burke D, Strathern J. 2005. *Methods in yeast genetics: a Cold Spring Harbor Laboratory course manual, 2005 ed*. Cold Spring Harbor Laboratory Press, Cold Spring Harbor, NY.

Asencio C, Chatterjee A, Hentze MW. 2018. Silica-based solid-phase extraction of cross-linked nucleic acid-bound proteins. *Life Sci Alliance* **1:** e201800088. doi:10.26508/lsa.201800088

Baejen C, Torkler P, Gressel S, Essig K, Soding J, Cramer P. 2014. Transcriptome maps of mRNP biogenesis factors define pre-mRNA recognition. *Mol Cell* **55:** 745–757. doi:10.1016/j.molcel.2014.08.005

Baleva MV, Meyer M, Entelis N, Tarassov I, Kamenski P, Masquida B. 2017. Factors beyond enolase 2 and mitochondrial lysyl-tRNA synthetase precursor are required for tRNA import into yeast mitochondria. *Biochemistry (Mosc)* **82:** 1324–1335. doi:10.1134/S0006297917110104

Baltz AG, Munschauer M, Schwanhausser B, Vasile A, Murakawa Y, Schueler M, Youngs N, Penfold-Brown D, Drew K, Milek M, et al. 2012. The mRNA-bound proteome and its global occupancy profile on protein-coding transcripts. *Mol Cell* **46:** 674–690. doi:10.1016/j.molcel.2012.05.021

Beckmann BM, Horos R, Fischer B, Castello A, Eichelbaum K, Alleaume AM, Schwarzl T, Curk T, Foehr S, Huber W, et al. 2015. The RNA-binding proteomes from yeast to man harbour conserved enigmRBPs. *Nat Commun* **6:** 10127. doi:10.1038/ncomms10127

Brannan KW, Jin W, Huelga SC, Banks CA, Gilmore JM, Florens L, Washburn MP, Van Nostrand EL, Pratt GA, Schwinn MK, et al. 2016. SONAR discovers RNA-binding proteins from analysis of large-scale protein-protein interactomes. *Mol Cell* **64:** 282–293. doi:10.1016/j.molcel.2016.09.003

Brimacombe R, Stiege W, Kyriatsoulis A, Maly P. 1988. Intra-RNA and RNA-protein cross-linking techniques in *Escherichia coli* ribosomes. *Methods Enzymol* **164:** 287–309. doi:10.1016/S0076-6879(88)64050-X

Castello A, Fischer B, Eichelbaum K, Horos R, Beckmann BM, Strein C, Davey NE, Humphreys DT, Preiss T, Steinmetz LM, et al. 2012. Insights into RNA biology from an atlas of mammalian mRNA-binding proteins. *Cell* **149:** 1393–1406. doi:10.1016/j.cell.2012.04.031

Cieśla M, Towpik J, Graczyk D, Oficjalska-Pham D, Harismendy O, Suleau A, Balicki K, Conesa C, Lefebvre O, Boguta M. 2007. Maf1 is involved in coupling carbon metabolism to RNA polymerase III transcription. *Mol Cell Biol* **27:** 7693–7702. doi:10.1128/MCB.01051-07

Darnell RB. 2010. HITS-CLIP: panoramic views of protein-RNA regulation in living cells. *Wiley Interdiscipl Rev RNA* **1:** 266–286. doi:10.1002/wrna.31

Dayon L, Hainard A, Licker V, Turck N, Kuhn K, Hochstrasser DF, Burkhard PR, Sanchez JC. 2008. Relative quantification of proteins in human cerebrospinal fluids by MS/MS using 6-plex isobaric tags. *Anal Chem* **80:** 2921–2931. doi:10.1021/ac702422x

Entelis N, Brandina I, Kamenski P, Krasheninnikov IA, Martin RP, Tarassov I. 2006. A glycolytic enzyme, enolase, is recruited as a cofactor of tRNA targeting toward mitochondria in *Saccharomyces cerevisiae*. *Genes Dev* **20:** 1609–1620. doi:10.1101/gad.385706

Franken H, Mathieson T, Childs D, Sweetman GMA, Werner T, Tögel I, Doce C, Gade S, Bantscheff M, Drewes G, et al. 2015. Thermal proteome profiling for unbiased identification of direct and indirect drug targets using multiplexed quantitative mass spectrometry. *Nat Protoc* **10:** 1567–1593. doi:10.1038/nprot.2015.101

Fuller GG, Han T, Freeberg MA, Moresco JJ, Ghanbari Niaki A, Roach NP, Yates JR III, Myong S, Kim JK. 2020. RNA promotes phase separation of glycolysis enzymes into yeast G bodies in hypoxia. *Elife* **9:** e48480. doi:10.7554/eLife.48480

Gerstberger S, Hafner M, Tuschl T. 2014. A census of human RNA-binding proteins. *Nat Rev Genet* **15:** 829–845. doi:10.1038/nrg3813

Glisovic T, Bachorik JL, Yong J, Dreyfuss G. 2008. RNA-binding proteins and post-transcriptional gene regulation. *FEBS Lett* **582:** 1977–1986. doi:10.1016/j.febslet.2008.03.004

Graczyk D, Ciesla M, Boguta M. 2018. Regulation of tRNA synthesis by the general transcription factors of RNA polymerase III: TFIIIB and TFIIIC, and by the MAF1 protein. *Biochim Biophys Acta* **1861:** 320–329. doi:10.1016/j.bbagrm.2018.01.011

Greenberg JR. 1979. Ultraviolet light-induced cross-linking of mRNA to proteins. *Nucleic Acids Res* **6:** 715–732. doi:10.1093/nar/6.2.715

Heinisch J. 1986. Construction and physiological characterization of mutants disrupted in the phosphofructokinase genes of *Saccharomyces cerevisiae*. *Curr Genet* **11:** 227–234. doi:10.1007/BF00420611

Hockensmith JW, Kubasek WL, Vorachek WR, von Hippel PH. 1986. Laser cross-linking of nucleic acids to proteins. Methodology and first applications to the phage T4 DNA replication system. *J Biol Chem* **261:** 3512–3518. doi:10.1016/S0021-9258(17)35677-6

Horos R, Büscher M, Kleinendorst R, Alleaume AM, Tarafder AK, Schwarzl T, Dziuba D, Tischer C, Zielonka EM, Adak A, et al. 2019. The small non-coding vault RNA1-1 acts as a riboregulator of autophagy. *Cell* **176:** 1054–1067.e1012. doi:10.1016/j.cell.2019.01.030

Hu WP, Chen YC, Chen WY. 2020. Improve sample preparation process for miRNA isolation from the culture cells by using silica fiber membrane. *Sci Rep* **10:** 21132. doi:10.1038/s41598-020-78202-8

Huang R, Han M, Meng L, Chen X. 2018. Transcriptome-wide discovery of coding and noncoding RNA-binding proteins. *Proc Natl Acad Sci* **115:** E3879–E3887. doi:10.1073/pnas.1718406115

Hughes CS, Foehr S, Garfield DA, Furlong EE, Steinmetz LM, Krijgsveld J. 2014. Ultrasensitive proteome analysis using paramagnetic bead technology. *Mol Syst Biol* **10:** 757. doi:10.15252/msb.20145625

Huppertz I, Perez-Perri JI, Mantas P, Sekaran T, Schwarzl T, Russo F, Ferring-Appel D, Koskova Z, Dimitrova-Paternoga L, Kafkia E, et al. 2022. Riboregulation of Enolase 1 activity controls glycolysis and embryonic stem cell differentiation. *Mol Cell* **82:** 2666–2680.e11. doi:10.1016/j.molcel.2022.05.019

Ignatiadis N, Klaus B, Zaugg JB, Huber W. 2016. Data-driven hypothesis weighting increases detection power in genome-scale multiple testing. *Nat Methods* **13:** 577–580. doi:10.1038/nmeth.3885

Jørgensen MG, Pettersen JS, Kallipolitis BH. 2020. sRNA-mediated control in bacteria: an increasing diversity of regulatory mechanisms. *Biochim Biophys Acta* **1863:** 194504. doi:10.1016/j.bbagrm.2020.194504

Kramer K, Sachsenberg T, Beckmann BM, Qamar S, Boon KL, Hentze MW, Kohlbacher O, Urlaub H. 2014. Photo-cross-linking and high-resolution mass spectrometry for assignment of RNA-binding sites in RNA-binding proteins. *Nat Methods* **11:** 1064–1070. doi:10.1038/nmeth.3092

Lee FCY, Ule J. 2018. Advances in CLIP technologies for studies of protein-RNA interactions. *Mol Cell* **69:** 354–369. doi:10.1016/j.molcel.2018.01.005

Love MI, Huber W, Anders S. 2014. Moderated estimation of fold change and dispersion for RNA-seq data with DESeq2. *Genome Biol* **15:** 550. doi:10.1186/s13059-014-0550-8

Lun AT, Smyth GK. 2016. csaw: a Bioconductor package for differential binding analysis of ChIP-seq data using sliding windows. *Nucleic Acids Res* **44:** e45. doi:10.1093/nar/gkv1191

Matia-Gonzalez AM, Laing EE, Gerber AP. 2015. Conserved mRNA-binding proteomes in eukaryotic organisms. *Nat Struct Mol Biol* **22:** 1027–1033. doi:10.1038/nsmb.3128

Mitchell SF, Parker R. 2014. Principles and properties of eukaryotic mRNPs. *Mol Cell* **54:** 547–558. doi:10.1016/j.molcel.2014.04.033

Mitchell SF, Jain S, She M, Parker R. 2013. Global analysis of yeast mRNPs. *Nat Struct Mol Biol* **20:** 127–133. doi:10.1038/nsmb.2468

Morawiec E, Wichtowska D, Graczyk D, Conesa C, Lefebvre O, Boguta M. 2013. Maf1, repressor of tRNA transcription, is involved in the control of gluconeogenetic genes in *Saccharomyces cerevisiae*. *Gene* **526:** 16–22. doi:10.1016/j.gene.2013.04.055

Pashev IG, Dimitrov SI, Angelov D. 1991. Crosslinking proteins to nucleic acids by ultraviolet laser irradiation. *Trends Biochem Sci* **16:** 323–326. doi:10.1016/0968-0004(91)90133-G

Perez-Perri JI, Rogell B, Schwarzl T, Stein F, Zhou Y, Rettel M, Brosig A, Hentze MW. 2018. Discovery of RNA-binding proteins and characterization of their dynamic responses by enhanced RNA interactome capture. *Nat Commun* **9:** 4408. doi:10.1038/s41467-018-06557-8

Perez-Perri JI, Noerenberg M, Kamel W, Lenz CE, Mohammed S, Hentze MW, Castello A. 2021. Global analysis of RNA-binding protein dynamics by comparative and enhanced RNA interactome capture. *Nat Protoc* **16:** 27–60. doi:10.1038/s41596-020-00404-1

Ponath F, Hör J, Vogel J. 2022. An overview of gene regulation in bacteria by small RNAs derived from mRNA 3′ ends. *FEMS Microbiol Rev* **46:** fuac017. doi:10.1093/femsre/fuac017

Queiroz RML, Smith T, Villanueva E, Marti-Solano M, Monti M, Pizzinga M, Mirea DM, Ramakrishna M, Harvey RF, Dezi V, et al. 2019. Comprehensive identification of RNA-protein interactions in any organism using orthogonal organic phase separation (OOPS). *Nat Biotechnol* **37:** 169–178. doi:10.1038/s41587-018-0001-2

Quendera AP, Seixas AF, Dos Santos RF, Santos I, Silva JPN, Arraiano CM, Andrade JM. 2020. RNA-binding proteins driving the regulatory activity of small non-coding RNAs in bacteria. *Front Mol Biosci* **7:** 78. doi:10.3389/fmolb.2020.00078

Ramírez F, Dündar F, Diehl S, Grüning BA, Manke T. 2014. deepTools: a flexible platform for exploring deep-sequencing data. *Nucleic Acids Res* **42:** W187–W191. doi:10.1093/nar/gku365

Ray D, Kazan H, Cook KB, Weirauch MT, Najafabadi HS, Li X, Gueroussov S, Albu M, Zheng H, Yang A, et al. 2013. A compendium of RNA-binding motifs for decoding gene regulation. *Nature* **499:** 172–177. doi:10.1038/nature12311

Scherrer T, Mittal N, Janga SC, Gerber AP. 2010. A screen for RNA-binding proteins in yeast indicates dual functions for many enzymes. *PLoS One* **5:** e15499. doi:10.1371/journal.pone.0015499

Schroeder A, Mueller O, Stocker S, Salowsky R, Leiber M, Gassmann M, Lightfoot S, Menzel W, Granzow M, Ragg T. 2006. The RIN: an RNA integrity number for assigning integrity values to RNA measurements. *BMC Mol Biol* **7:** 3. doi:10.1186/1471-2199-7-3

Shchepachev V, Bresson S, Spanos C, Petfalski E, Fischer L, Rappsilber J, Tollervey D. 2019. Defining the RNA interactome by total RNA-associated protein purification. *Mol Syst Biol* **15:** e8689. doi:10.15252/msb.20188689

Singh R, Green MR. 1993. Sequence-specific binding of transfer RNA by glyceraldehyde-3-phosphate dehydrogenase. *Science (New York, NY)* **259:** 365–368. doi:10.1126/science.8420004

Singh G, Pratt G, Yeo GW, Moore MJ. 2015. The clothes make the mRNA: past and present trends in mRNP fashion. *Annu Rev Biochem* **84:** 325–354. doi:10.1146/annurev-biochem-080111-092106

Suchanek M, Radzikowska A, Thiele C. 2005. Photo-leucine and photo-methionine allow identification of protein-protein interactions in living cells. *Nat Methods* **2:** 261–268. doi:10.1038/nmeth752

Szatkowska R, Garcia-Albornoz M, Roszkowska K, Holman SW, Furmanek E, Hubbard SJ, Beynon RJ, Adamczyk M. 2019. Glycolytic flux in *Saccharomyces cerevisiae* is dependent on RNA polymerase III and its negative regulator Maf1. *Biochem J* **476:** 1053–1082. doi:10.1042/BCJ20180701

Trendel J, Schwarzl T, Horos R, Prakash A, Bateman A, Hentze MW, Krijgsveld J. 2019. The human RNA-binding proteome and its dynamics during translational arrest. *Cell* **176:** 391–403.e319. doi:10.1016/j.cell.2018.11.004

Tsvetanova NG, Klass DM, Salzman J, Brown PO. 2010. Proteome-wide search reveals unexpected RNA-binding proteins in *Saccharomyces cerevisiae*. *PLoS One* **5:** e12671. doi:10.1371/journal.pone.0012671

Ule J, Hwang HW, Darnell RB. 2018. The future of cross-linking and immunoprecipitation (CLIP). *Cold Spring Harb Perspect Biol* **10:** a032243. doi:10.1101/cshperspect.a032243

Upadhya R, Lee J, Willis IM. 2002. Maf1 is an essential mediator of diverse signals that repress RNA polymerase III transcription. *Mol Cell* **10:** 1489–1494. doi:10.1016/S1097-2765(02)00787-6

Urdaneta EC, Vieira-Vieira CH, Hick T, Wessels HH, Figini D, Moschall R, Medenbach J, Ohler U, Granneman S, Selbach M, et al. 2019. Purification of cross-linked RNA-protein complexes by phenol-toluol extraction. *Nat Commun* **10:** 990. doi:10.1038/s41467-019-08942-3

Van Nostrand EL, Pratt GA, Shishkin AA, Gelboin-Burkhart C, Fang MY, Sundararaman B, Blue SM, Nguyen TB, Surka C, Elkins K, et al. 2016. Robust transcriptome-wide discovery of RNA-binding protein binding sites with enhanced CLIP (eCLIP). *Nat Methods* **13:** 508–514. doi:10.1038/nmeth.3810

Willis IM. 2018. Maf1 phenotypes and cell physiology. *Biochim Biophys Acta* **1861:** 330–337. doi:10.1016/j.bbagrm.2017.11.009

MEET THE FIRST AUTHOR

Claudio Asencio

***Meet the First Author(s)* is an editorial feature within *RNA*, in which the first author(s) of research-based papers in each issue have the opportunity to introduce themselves and their work to readers of *RNA* and the RNA research community. Claudio Asencio is the first author of this paper, "Small noncoding RNA interactome capture reveals pervasive, carbon source–dependent tRNA engagement of yeast glycolytic enzymes." Claudio was formerly a visiting researcher in Dr. Matthias W. Hentze's laboratory at the European Molecular Biology Laboratory (EMBL), and is currently a senior research associate at the Genomics Core Facility at EMBL. Claudio's research focuses on developing new methods and technologies enabling multiomics analysis of single cells and ultra-low input samples with direct application for the study of human diseases.**

What are the major results described in your paper and how do they impact this branch of the field?

Previous work at Dr. Hentze's laboratory resulted in the development of the 2C method, which facilitates the enrichment and detection of UV-crosslinked RNA–protein complexes. In that publication, we proposed that 2C could be the base for the implementation of different methods impacting the identification and characterization of RNA–protein interactions. Following those ideas, we describe in this paper the development of methods derived from 2C, which greatly facilitate the study of RNA–protein complexes. This includes RIC_{2C} for the identification of the total RNA-binding proteome and $CLIP_{2C}$, for the identification of the target RNA molecules bound by a specific RBP. Particularly relevant was the development of $snRIC_{2C}$, enabling for the first time, the identification of proteins binding specifically to small noncoding RNAs. In addition, the development of these methods resulted in interesting biological observations, like the detection of multiple glycolytic enzymes moonlighting as snRNA-binding proteins. Overall, the unique combination of methodological advances coupled with relevant biological insight, makes this paper of interest for the broad RNA research community.

What led you to study RNA or this aspect of RNA science?

I worked on proteins related to energy metabolism during my PhD. This not only included understanding their direct role in energy metabolism, but also additional functions, like their effect on cellular homeostasis and ageing. Therefore, I found fascinating the research work conducted at Dr. Hentze's laboratory, pioneering the study of the dual role of many of these metabolic enzymes, moonlighting as RNA-binding proteins.

I feel privileged for contributing to the field with the development of methods enabling and/or simplifying the identification and characterization of these RBPs. I am particularly excited about the development of $snRIC_{2C}$, as the identification of proteins binding to snRNA was usually not achieved by conventional RNA interactome capture methods.

During the course of these experiments, were there any surprising results or particular difficulties that altered your thinking and subsequent focus?

Several glycolytic enzymes were previously identified as RBPs, like human GAPDH, known to bind to tRNAs. However, it was very surprising to identify additional multiple proteins along the glycolytic pathway and mitochondrial TCA cycle to moonlight specifically as snRNA-binding proteins. The biological relevance of these interactions is far from being understood. But beautiful examples, like the control of glycolysis and embryonic stem cell differentiation by the riboregulation of Enolase 1 and the regulation of autophagy by the snRNA Vault RNA1-1 suggests that an exciting entire scientific field is waiting to be explored.

What are some of the landmark moments that provoked your interest in science or your development as a scientist?

I have always had a very curious mind and I was always very excited to learn new things. It could be about machines, space, physics or

Continued

nature. It did not matter, but it was just a genuine interest in knowing how things work. However, I still remember a fantastic and influential Biology teacher at High School, who helped me realize that my actual passion is biology and its universe of incredibly small machines that make life possible.

If you were able to give one piece of advice to your younger self, what would that be?

Think out of the box! The development of 2C and its derived methods came as an idea to significantly simplify current methods for the isolation or enrichment of UV-crosslinked RNA-binding proteins. That simple idea resulted in the development of several novel methods and the discovery of multiple metabolic enzymes moonlighting as snRBPs.